Combining Distance and Force Measurements to Monitor the Usage of Walker Assistive Devices

J.M. Dias Pereira[1,2], Vítor Viegas[1,2]
(1) LabIM ESTSetúbal/IPS,
Escola Superior de Tecnologia de Setúbal do Instituto Politécnico de Setúbal, Setúbal, Portugal
(2) Instituto de Telecomunicações, Lisbon, Portugal

Octavian Postolache[2,3], Pedro Silva Girão[2,4]
(2) Instituto de Telecomunicações, Lisbon, Portugal
(3) ISCTE-IUL, Lisbon, Portugal
(4) DEEC/Instituto Superior Técnico, Lisbon, Portugal

***Abstract*—This paper presents a measurement system that can be used to monitor the usage of walker assistive devices. The forces applied on the legs of the walker device are measured using low cost force sensing resistors and a light detection and ranging device is used to evaluate several gait kinematic parameters, such as, walking speed and walking stride length. To evaluate the right usage of the walker device two walker indexes, one related with the applied forces and the other related with walker gait phases, are introduced. The measurement system includes wireless communication capabilities that enable a local and remote supervision of the measuring data.**

***Keywords*—walker assistive device; force measurements; distance measurements; kinematic parameters; walker risk indexes**

I. Introduction

Topics related with people mobility are already of major importance today and this importance will be even greater in the near future. Not only for patients, during recovery periods, but also, and above all, for elderly people, the usage of assistive walking devices can extend significantly their autonomy and quality of life. Regarding statistics and previsions, it is estimated that by 2025 in United States and Canada 25 % of the population will be aged over 65 years older [1-3]. Moreover, it is expected that in the European Union, for year 2060, the life expectance for women and men will be around 89 and 84.5 years, respectively [4]. In this context, it is important to refer that a proper usage of mobility aiding devices by elderly people can provide significant cost savings of health and long-term care systems [5-7]. However, it must be underlined that harmful injuries [8-9] can result from a bad usage of mobility aiding devices, being important to monitor its right usage. Thus, it is important to develop measurement solutions that can be used to monitor balance and stability conditions of users of mobility aiding devices. Several authors already studied measurement solutions for this purpose [10-14] but some solutions are complex, expensive and the added value of the additional information that can be accessed is questionable in terms of walker day-by-day applications. Moreover, several alternative systems include accelerometer sensors to extract kinematic parameters, like the ones related with human gait, and those sensors require the usage of complex algorithms to improve measurement data accuracy [15-16].

The main novelties that can be mentioned in the proposed measurement systems includes its low cost and easy adaptability to existing walker devices, the capability to extract kinematic parameters based on optical distance measurements, the capability to detect unbalance conditions and to detect, in real time, potential falling conditions. To obtain the experimental data, a prototype, based on a conventional walker with a four legs ground contact configuration, was implemented and used for testing purposes. It is important to refer that the measurement methods and technical solutions that are presented can be easily be applied to others mobility aiding devices, particularly, walkers with different ground contact configurations, namely wheeled walkers and rollators.

The paper is organized as follows: section two presents the proposed measurement solution and novelties; section three includes the hardware and software description of the measurement system; section four includes the experimental results and the last section, section five, draws the conclusions.

II. Proposed Measurement Solution and Novelties

Considering the Cartesian plane associated with the coordinates of the pick-up walker legs, represented in Fig. 1, the center of pressure (COP) of the set of the four forces, each one associated with one leg of the walker device, is given by [17]:

$$COP_X = \frac{W_{12}\cdot(F_{L1}-F_{L2})+W_{34}\cdot(F_{L3}-F_{L4})}{2\cdot(F_{L1}+F_{L2}+F_{L3}+F_{L4})}$$
$$COP_Y = \frac{L\cdot[(F_{L1}-F_{L3})+(F_{L2}-F_{L4})]}{2\cdot(F_{L1}+F_{L2}+F_{L3}+F_{L4})} \quad (1)$$

where F_{Lk} represents the force applied in each walker leg, W_{12} and W_{34}, represent the distances between the pair of rear and front walker legs, respectively, that corresponds approximately to the walker width (W), and L represents the distance between the rear and front walker legs, that corresponds to the walker length.

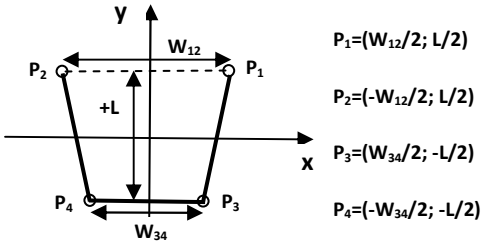

Fig. 1. Cartesian plane associated with the coordinates of the pick-up walker legs (L- distance between front and rear legs, W_{12}- distance between rear legs, W_{34}- distance between front legs).

The normalized deviation of the COP coordinates from the geometrical center of the polygon defined by the floor contacts of the walker legs can be used to define the following walker risk index:

$$WRI_1 = 100 \cdot \frac{\sqrt{(COP_X)^2+(COP_Y)^2}}{\sqrt{(W/2)^2+(L/2)^2}} \cdot \alpha_{FW} \ \% \qquad (2)$$

where W and L represent the mean value of the walker width and the walker length, respectively, and (α_{FW}) is a weighting factor, defined by:

$$\alpha_{FW} = \frac{F_{L1}+F_{L2}+F_{L3}+F_{L4}}{WU_w} \qquad (3)$$

where WU_w represents the walker user weight and the numerator of the fraction represents the total force applied on the walker legs. The value of this factor varies between 0 and 1 and its maximum value corresponds to the limit situation that would occur if all the weight of the walker user was applied on the four walker legs.

A second parameter that can be used to evaluate the right usage of the walker device, and that can be measured by another walker risk index (WRI_2), can be defined in terms of the synchronization between walker movements and user gait. Fig. 2(a) represents the walker step-to gait phases that occur in a correct usage of the walker device and Fig. 2(b) represents the state machine diagram that is associated with the step to gait phases. The continuous arrows are associated with normal gait state transitions and the dotted arrows are associated with abnormal gait state transitions.

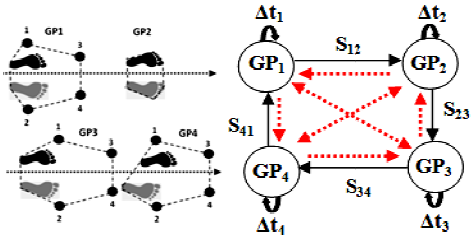

(a) (b)

Fig. 2. Gait phases: (a) walker step to gait phases (black foot print- affected foot; gray foot print- unaffected foot; dashed polygon- base of support limits; black circles- walker leg floor contact; dotted line - walking line of progression); (b) state machine diagram associated with the step to gait phases (continuous arrows- normal state transitions; dotted arrows- abnormal state transitions).

Since, the transitions between the stable states are validated by the sensor outputs, that include the set of the four force sensing resistors (FSR) and the optical light detection and ranging (LIDAR) distance sensor, it is possible to validate correct and incorrect phase transitions during walker usage. If N_{12}, N_{23}, N_{34} and N_{41}, represent the number of normal state transitions associated with S_{12}, S_{23}, S_{34} and S_{41}, respectively, WRI_2, can be defined by:

$$WRI_2 = \sum_{n=1}^{nsteps} 100 \cdot \left(\frac{N_{12}+N_{23}+N_{34}+N_{41}}{N_{total}} \right) \% \qquad (4)$$

where nsteps represents the number of steps that is used to evaluated the WRI_2, and N_{total}, represents the total number, normal and abnormal, state transitions. The coefficient nsteps is configured by software and its default value is equal 10. However, higher or lower values can be used, existing, obviously, a compromise between the promptness of the detection of risk events and their statistical meaning. The sum of the four temporization, $\Delta t1$ till Δt_4, signalized in the state diagram, corresponds to the step duration.

The gray circles represented in Fig. 3 identifies the four gait phases and the force and distance conditions that are use to increment the counter (N_{ij}) that is associated with correspondent state transition (S_{ij}).

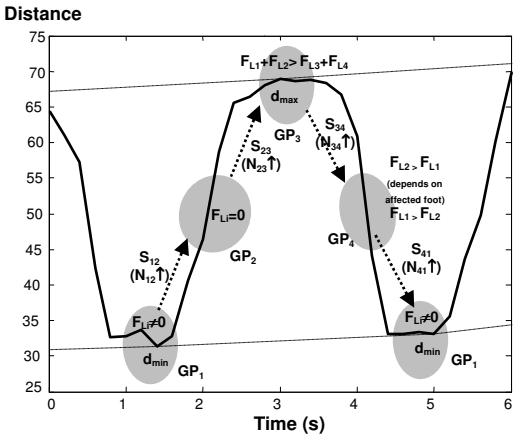

Fig. 3. Increment of state transition counters ($N_{ij}\uparrow$) during the four walker gait phases (gray circles).

III. Measurement System

The main elements of the measurement system includes a set of four sensing resistors, an optical distance sensor, the associated signal conditioning circuits, and the data acquisition and transmission units. The pick-up standard walker that was used for testing purposes [18] has the following main characteristics: width between rear legs (W_{12}) equal to 52 cm, width between front legs (W_{34}) equal to 51 cm, length between front and rear legs (L) equal to 45 cm and a height adjustability between 78 cm and 90 cm, in increments of 2.5 cm.

The wireless communication that supports the connection between the measurement system that is installed on the walker device, and a remote Tablet PC, is based on a Bluetooth-TTL transceiver module [19]. These hardware modules were designed and successfully tested by the authors in previous applications [20] and could be integrated in the future in single Arduino or Raspberry platform.

A. Hardware

Fig. 4 depicts the positioning of the sensing units in the developed prototype. As it is clearly visible there are no restrictions that interfere with the user movements and the additional weight caused by integration of the measurement system is lower than 200 gf, being almost half of the total weight associated with the battery pack module.

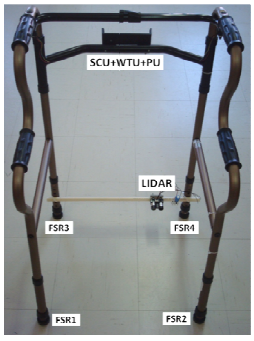

Fig. 4. Positioning of the sensing units in the four leg walker device (FSR- force sensing resistor; LIDAR- light detection and ranging unit; SCU+WTU+PU- signal conditioning, wireless transmission and power units).

A.1 Force sensing resistors

A low-cost polymer thick film device was used as a force sensing element [21]. The main characteristics of the FSR include a measuring force range of 100 lb (FS), a linearity error lower than 3% of FS, a repeatability better than 2.5% of full scale (FS), a hysteresis lower than 4.5% of FS and a response time lower than 5 µs. The schematic diagram of the circuit that was used for signal conditioning is represented in Fig. 5. A JFET [22] input operational amplifier was used in order to take advantage of its low values of bias and offset currents that are equal to 30 pA and 3 pA, respectively.

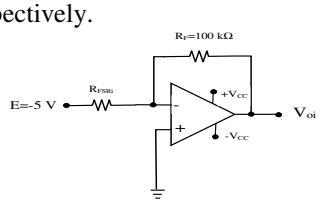

Fig. 5. Basic current to voltage converter circuit used for signal conditioning of the FSR sensors.

Assuming an ideal behavior of the OPAMP circuit, and a linear variation of the conductance of the FSR with force amplitude, the output voltage V_{0i}, associated with each FSR, is given by:

$$V_{0i}=-E\cdot R_F\cdot(G_{0i}+m_i\cdot F_i) \quad (5)$$

where G_{0i} and m_i are the coefficients of the linear variation of the conductance of each FSR with force. An important issue that must be referred is that it is essential to characterize each FSR according to their real usage conditions. Thus, each FSR was calibrated using the same mechanical fixture that was used for its connection with the walker leg (see Fig. 6).

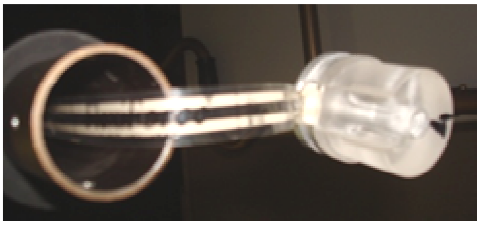

Fig. 6. Detail of the mechanical fixture that was used to connect the FSR with the walker leg.

The calibration of each FSR was performed applying force amplitudes that vary between 0 and 10000 gf. A precision balance, with an accuracy better than 20 gf [23], was used to measure the force amplitude. Fig. 7 represents the results that were obtained in the calibration of each FSR. Since the resistance of every FSR is always higher that 50 MΩ when no force is applied on the sensor, the linear interpolation of the conductance (G_{FSR}) values, that was performed, considered that the linearized conductance characteristic passes through the origin of the graph. As it can be easily verified, from the experimental results, the maximum ratio between the sensitivity coefficients (m), of the different FSR, can be as high as 3.5, which confirms that it is essential to perform an individual calibration of each FSR.

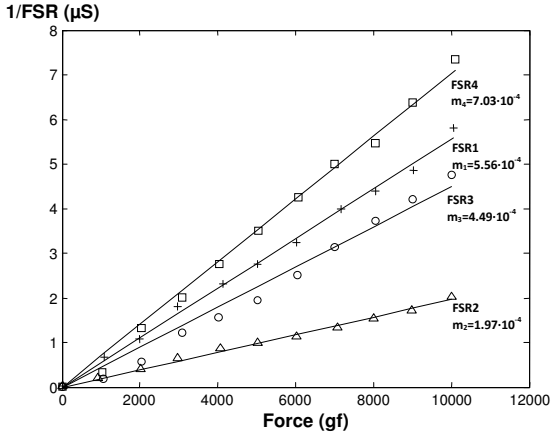

Fig. 7. FSR calibration results (m represent the straight line slope in µS/gf).

A.2 LIDAR

A low-cost LIDAR device [24] was used to perform the optical distance measurements. The LASER, that is associated with this device, uses pulsed light and modulated signals to improve the measurement accuracy. The main characteristic of the LIDAR device includes a working wavelength of 905 nm, a maximum pulse train length of 256 pulses, a pulse repetition rate of 20 kHz, an accuracy better than 2.5 cm, a measurement range that can achieve 40 m, much higher than the required value for our application, an I2C communication interface and a PWM output signal with a 10 µs resolution. The theoretical relation between the pulse duration (Ton) and the distance is given by:

$$D=0.1\cdot Ton \quad (6)$$

where D represents distance to be measured in cm and Ton represents the pulse duration of the PWM signal in µs.
Fig. 8 represents the experimental setup that was used to perform the characterization of the LIDAR sensor. As represented in Fig. 8, a plotter [25] with an accuracy of 0.25% of effective recording span was used to characterize the optical sensor. The positioning accuracy of the plotter is better than 0.5 mm when using its 50 mV/cm input voltage range.

Fig. 8. Experimental setup that was used to characterize the optical sensor.

Since the frequency of the measuring signal is much lower than the LIDAR acquisition rate, it is enough to perform a static characterization of the device. Fig. 9 represents the calibration results that were obtained, for a measuring range between 10 and 100 cm.

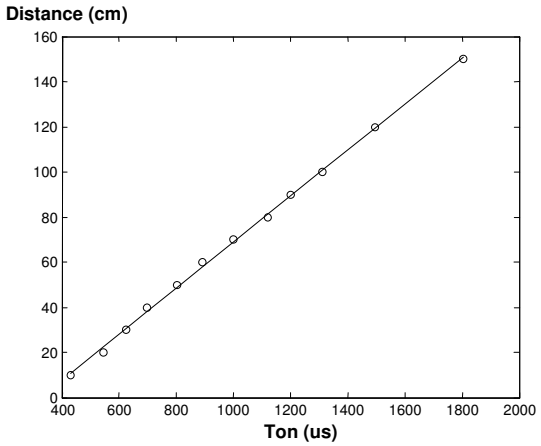

Fig. 9. Static characterization results of the LIDAR device for distance varying between 10 and 100 cm.

Using a linear interpolation, the following relationship between distance and Ton is obtained:

$$D=0.1020 \cdot Ton-33.04 \quad (7)$$

The offset error between theoretical and experimental results can easily be cancelled and results from the zero reference position of the LIDAR that is not equal to the one that was used for calibration purposes.

B. *Software*

Several MATLAB and LabVIEW software routines were developed for data acquisition and signal processing of measurement data. The software includes routines for measurement system calibration, storage of historical data and extraction of gait pattern parameters that are obtained from the force and distance sensors. Routines to detect unbalance conditions, walker risk indexes and gait phases identification, as well as the extraction of walking kinematic parameters, were also developed. The configuration of the measurement system include the following main parameters: age, height and weight of the walker user, number of measurement channels, data acquisition rate, criteria used to define walker risk indexes and warnings of potential unbalance conditions. A particular attention was dedicated to the software routine that was used to detect the maximum and minimum distance values in order to remove measurement data outliers and to evaluate correctly the walking kinematic parameters, such as, walking step length and walking speed. The peak detection function that was developed preserve the main features of the basic MATLAB *findpeaks* function but the slope and amplitude thresholds parameters, as well as, smooth and fit width parameters, were constrained to the expectable limit values of the walking measurement data. Simple filtering signal processing routines were not used because some important gait patterns details could be lost and the temporal relation between distance and force signals must be preserved for a correct identification of the gait phase transitions.

IV. Experimental Results

Several experimental results were performed with the walker prototype that was developed for testing purposes. The sensors were easily integrated in a commercial walker device without need of any modification in its mechanical structure. The FSR were installed in the terminal part of each walker leg with an appropriate fixture that was inserted inside the walker leg rubber. The optical distance sensor was fixed in the frontal frame bar of the walker and the measuring beam was adjusted towards the walker user leg.

A. *FSR tests*

Using the calibration coefficients of the FSR, it is possible to obtain a real time measurement of the forces that are applied in each walker leg. As an example, Fig. 10 represents the intensity of the forces in each walker leg when the walker user simulates a gait pattern with a right affected foot. As it is clearly visible in the figure the intensity of the forces are higher on the left pair of legs of the walker (F_{LEG1} and F_{LEG3}), being the force on the rear leg (F_{LEG1}) a little bit higher than the force on front leg (F_{LEG3}). These results were expected since the compression forces are greater in the opposite side of the affected foot [26].

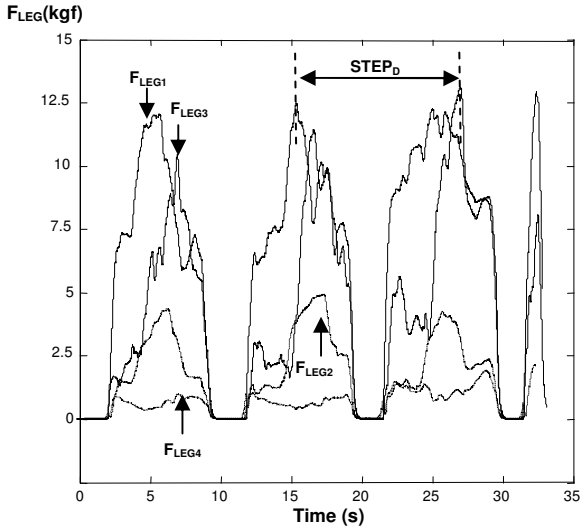

Fig. 10. Intensity of the forces in each walker leg when the walker user simulates a gait pattern with a right affected foot.

Fig. 11 represents the variation of the walker risk index 1 (WRI_1) for the set of forces previously represented. From the distance measurements, it can be confirmed that the walker risk index (WRI_1) is maximum when the walker user advances its unaffected foot and applies maximum forces on the left side of the walker.

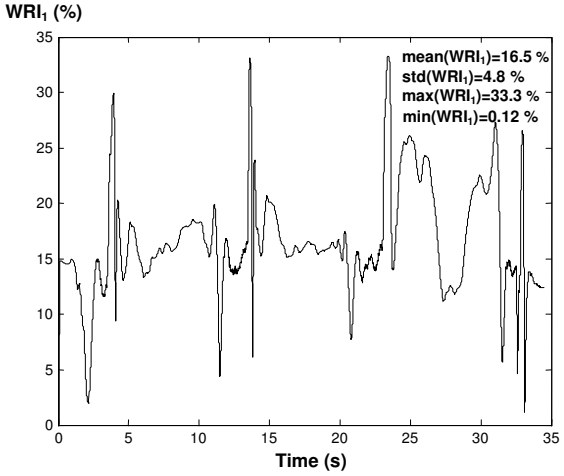

Fig. 11. Variation of the WRI_1 for the set of forces represented in Fig. 10 (the walker user simulates a gait pattern with a right affected foot).

B. LIDAR tests

Regarding the optical distance measurements, Fig. 12 and Fig. 13 represent the distance measurement data, and the associated step lengths, for a walker gait that contains 18 steps. A correct evaluation of the maximum and minimum distance values, for each step, was successfully achieved for different walking patterns after a right adjustment of the parameters of the *findpeaks* MATLAB function.

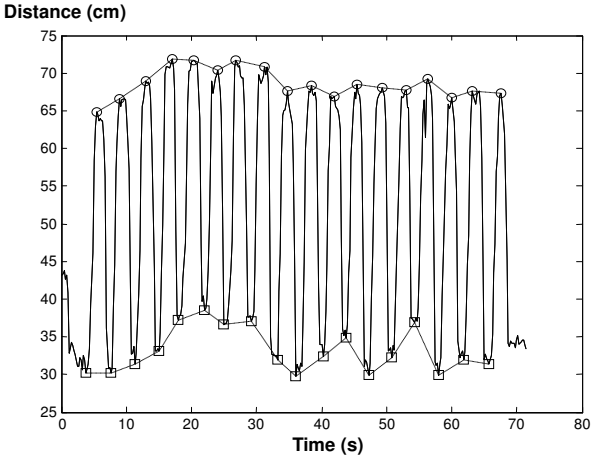

Fig. 12. Distance measurement values for a walker gait that contains 18 steps (○- maximum distances; minimum distances).

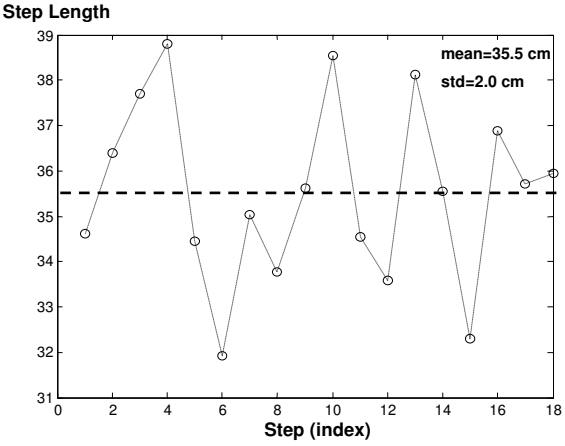

Fig. 13. Step lengths of the walker gait represented in the previous figure.

In order to compare the kinematic parameters that are obtained with different walking patterns, a second test was performed simulating a regular and an irregular walking pattern. The results, regarding the maximum and minimum distances values, obtained for each simulated walking pattern, are represented in Fig. 14 and Fig. 15. It is clearly visible from the results that the standard deviation of the step lengths are much higher in the simulated irregular walking pattern. In this example the ratio of the standard deviations of the maximum and minimum distances, associated with each walking pattern, are approximately equal to two and five, respectively.

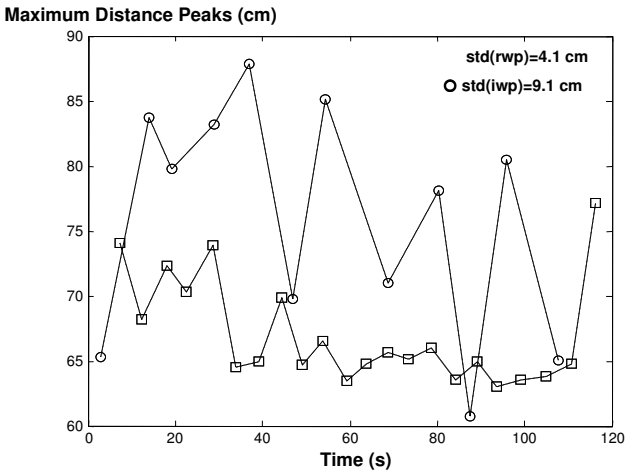

Fig. 14. Maximum distance measurement values for walker gaits with two different patterns (○- irregular pattern; regular pattern).

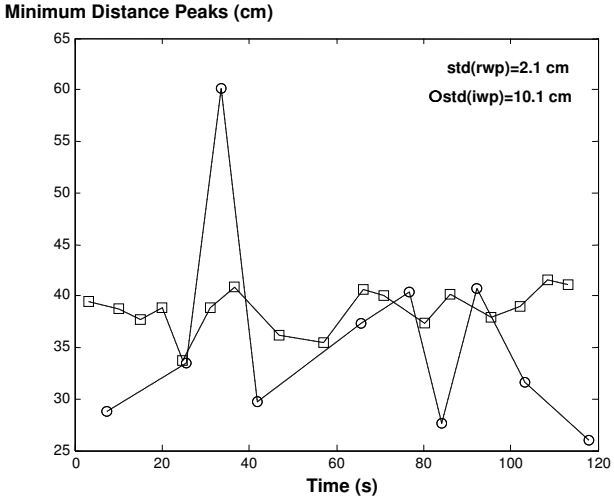

Fig. 15. Minimum distance measurement values for walker gaits with two different patterns (○- irregular pattern; regular pattern).

Thus, the average value and the standard deviation of the maximum and minimum values of step lengths are, among others, two important parameter that can be used to classify the walker gait patterns. Other important parameter that can be easily accessed by the proposed measurement system, is based on the synchronization between walker and feet movements of the walker user that define proper evolution of the gait phases.

V. CONCLUSIONS

The experimental results that were obtained confirm that it is possible to monitor the right usage of walker assistive devices combining the measurement data from FSR and optical distance sensors. Using wireless transmission capabilities and the Internet, it is possible to use the proposed measurement system with patients that need to learn how to use correctly walker devices or to remotely supervise people that use regularly walker devices at home. Finally, it is important to refer that, although, the present paper assumes that a basic walker is used, the proposed measurement solution can be easily applied to other types of walker assistive devices, with appropriate adaptations. Future research work will be done in order to consider additional walker risk indexes related with physiologic demands, such as, the increase of user heart

rate or the increase of the oxygen consumption, that occur during the usage of every walker assistive device and additional field tests, with elderly people and patients with different diseases, are required to set a fine tuning between the walker risk indexes values and potential falling risks associated with loss of stability. It must also be underlined that besides centralized data processing of measurement data, self-warnings and alarms can also be signalized in the walker device if the walker indexes are out of their acceptance range, in terms of stability limits, or if their trend values are moving away from their average values, obtained from historical data.

ACKNOWLEDGEMENT

The work was supported by Fundação para a Ciência e Tecnologia project: PTDC/DTP-DES/6776/2014, by Instituto de Telecomunicacões and by ESTSetúbal/IPS. A special acknowledgement goes to the Erasmus student Achille Maingot that collaborated in the laboratory characterization of the LIDAR device.

REFERENCES

[1] Carrie A. Werner (2010). "The Older Population: 2010" (PDF). 2010 Census Briefs. U.S. Census Bureau. C2010BR-09.

[2] Taylor, Albert W.; Johnson, Michel J. (2008). Physiology of Exercise and Healthy Aging. Human Kinetics. ISBN 978-0-7360-5838-4.

[3] "Population". 2008 Older Americans : Key indicators of Well-Being. 2008.

[4] European Commission, "Summaries of EU Legislation", Available at: http://europa.eu/legislation_summaries/employment_and_social_policy/situation_in_europe/c10160_en.htm [accessed Sept. 2014].

[5] S.R.Faruqui, T. Jaeblon," Ambulatory assistive devices in orthopaedics: uses and modifications", J Am Acad Orthop Surg. Issue 18, No. 1, p.p. 41–50, 2010.

[6] H. Bateni, B.E. Maki, "Assistive devices for balance and mobility: benefits, demands, and adverse consequences", Arch Phys Med Rehabil, Issue 86, No. 1, pp. 134–145, 2005.

[7] NTT data, Global IT Innovator, "Trends in Telehealth", Available at: http://americas.nttdata.com/Industries/Industries/Healthcare/~/media/Documents/White-Papers/Trends-in-Telehealth-White-Paper.pdf [accessed Sept. 2014].

[8] H. Bateni, B.E. Maki, "Assistive devices for balance and mobility: benefits, demands, and adverse consequences", Arch Phys Med Rehabil, Issue 86, No. 1, pp. 134–145, 2005.

[9] J.A. Stevens, K. Thomas, L. Teh, Greenspan et al, "Unintentional fall injuries associated with walkers and canes in older adults treated in U.S. emergency departments", J Am Geriatr Soc. Issue 57, No. 8, pp. 1464–1469, 2009.

[10] D.D. Ely, G.L. Smidt, "Effect of Cane on Variables of Gait for Patients with Hip", Phys. Ther., No. 57, pp. 507-512, 1977.

[11] Majd Alwan et al., "basic Walker-Assisted gait Characteristics Derived from Forces and Moments Exerted on the Walker's Handles: results on normal subjects", Medical Engineering and Physics, No. 29, pp. 380-389, 2007.

[12] Alvaro Muro-de-la-Herran, Begonya Garcia-Zapirain and Amaia Mendez-Zorrilla, " Gait Analysis Methods: An Overview of Wearable and Non-Wearable Systems, Highlighting Clinical Applications", Sensors Review, 14, pp. 3362-3394, 2014.

[13] Joel A. Delisa, Department of Veteran Affairs, "Rehabilitation Reserach and Development Service", Chapter 2, pp. 11-32, 1981.

[14] E.Sardini, M. Serpelloni, M. Lancini, Wireless Instrumented Crutches for Force and Movement Measurements for Gait Monitoring", IEEE Transaction on Instrumentation and Measurement, Vol. 64, No. 12, pp. 3369-3379, Dec. 2015.

[15] S.K. Keadle, E.J. Shirom, P.S. Freedson, I.M. Lee, "Impact of accelerometer data processing decisions on the sample size, wear time and physical activity level of a large cohort study", BMC Public Health, 14:1210, 2014.

[16] I.M. Lee, E.J. Shiroma, " Using accelerometers to measure physical activity in large-scale epidemiological studies: issues and challenges", Br J Sports Med., 48(3), pp. 197-201., Feb. 2014.

[17] J.M. Dias Pereira, Octavian Postolache, Vítor Viegas, Pedro Silva Girão , "A Low Cost Measurement System to Extract Kinematic Parameters from Walker Devices", Instrumentation and Measurement Technology Conference (I2MTC), Vol. 1, pp. 1991-1996, 2015.

[18] Ayudas Dinâmicas, Model AD232. Available at: http://www.ayudasdinamicas.com/caminador-de-incorporacion/ [accessed Oct. 2016].

[19] MDFLY Electronics, Wireless Bluetooth TTL Transceiver Module. Available at: http:// www.mdfly.com [accessed Sept. 2014].

[20] J.M. Dias Pereira, Vítor Viegas, Octavian Postolache, Pedro Silva Girão, "A Smart and Distributed Measurement System to Acquire and Analyze Mechanical Motion Parameters", Metrology and Measurement Systems, Vol. 20, No. 3, pp. 465-478, 2013.

[21] Interlink Electronics, "Force Sensing Resistors: integration guide and evaluation parts catalog", Available at: http://www.interlinkelectronics.com [accessed Sept. 2014].

[22] Texas Instruments, LFx5x JFET Input Operational Amplifiers. Available at: http://www.ti.com/lit/ds/symlink/lf357.pdf [accessed Oct. 2016].

[23] Mettler-Toledo Gmbh, "Mettler Toledo Spider 1S Scales", Switzerland, 1999.

[24] Pulsed Lite LLC, "LIDAR-Lite, Silver Label". Available: https://github.com/PulsedLight3D [accessed Oct. 2016].

[25] Yokogawa Hokushin Electric, YEW Model 3025 A4 X-Y Recorder. Available at: http://www.electro-meters.com/yokogawa/yokogawa-recorders/3025-2/ [accessed Oct. 2016].

[26] Kevin McQuade, M. Finley, A. Oliveira, "Upper Extremity Joint Stresses During Walker-Assisted Ambulation in Post-Surgical Patients", Revista Brasileira de Fisioterapia, Vol. 15, No.4, pp. 332-337, July/Aug. 2011.